Molecular Dynamics of Generation Process of Double-Walled Carbon Nanotubes from Peapods

Yasushi Shibuta[1] and Shigeo Maruyama[2]

[1]Department of Materials Engineering, The University of Tokyo, Japan

[2]Department of Mechanical Engineering, The University of Tokyo, Japan

Abstract

The generation process of a double-walled carbon nanotube (DWNT) from a "peapod" was studied by classical molecular dynamics simulation. Starting from a peapod structure, defined by five C_{60} molecules inside a (10,10) single-walled carbon nanotube (SWNT), polymerized fullerenes, a peanut-like structure and an almost nanotube-like structure were obtained under suitable conditions of temperature control. The mean distance between the two layers of the DWNT agreed with an experimental report that it is larger than the interlayer spacing found in multi-walled carbon nanotubes (MWNTs). In addition, the chirality dependence of the potential energy of a DWNT on the relative chirality of its constituent tubes was examined using a 6-12 Lennard-Jones potential. It was found that the potential energy depends only on the distance between the two layers, not on the relative chiralities.

Key words: Molecular Dynamics Method, Double-walled Carbon Nanotubes, Peapods.

1. Introduction

The recognition of multi-walled carbon nanotubes (MWNTs) [1] in 1991, and single-walled carbon nanotubes (SWNTs) [2] in 1993, opened up a new research area for these novel carbon materials. Several remarkable mechanical and electrical properties of SWNTs have been revealed so far, such as a metal-semiconductor duality determined by the chiral number (*n*,*m*) that is uniquely assigned to each chiral structure of SWNTs [3]. At first, the synthesis of SWNTs was carried out with a pulsed laser-oven technique using a Ni/Co-doped graphite rod [4] or an electric arc-discharge technique using a Ni/Y-doped graphite rod [5]. However, more recently, the catalytic chemical vapor deposition (CCVD) technique has been extensively investigated [6] due to its potential for more large-scale production of SWNTs. We have developed a high-purity production technique for SWNTs using a low-temperature alcohol CCVD method [7-11].

Smith *et al.* [12] discovered encapsulated C_{60} in SWNTs synthesized by a laser-oven technique and named it these structures “peapods”. They ware made by a purification process using nitric acid and subsequent annealing of SWNTs synthesized by the laser-oven technique. The SWNTs were damaged and made defective by the nitric acid, and the fullerenes subsequently synthesized were encapsulated in the annealing process. Since then, a high-purity production technique for peapods was developed by adding sublimated fullerenes to purified SWNTs [14-16], and it enabled the encapsulation of C_{70} [15,16], Gd@C_{82} [17] and other small fullerenes. The physical and optical properties of peapods have been studied using electron diffraction [16,17] and Raman spectroscopy [15,19]. In particular, it was observed that encapsulated fullerenes coalesced and formed a double-walled carbon nanotube (DWNT) [12,18], and that DWNTs could also be made by heat treatment of peapods about 1200 °C

[14,19]. Interestingly, transmission electron microscope images and Raman spectra showed that the mean distance between the inner and outer tube in DWNTs was about 3.6 Å; that is, about 6% wider than interlayer spacings found in MWNTs or turbostratic graphite (both about 3.4 Å) [19]. It is also interesting how the diameter and chirality of inner tube is determined depending on that of outer tube. In addition, the high-temperature pulsed arc discharge [20] and the CCVD method [21] enabled selective synthesis of DWNTs. For a better understanding of formation mechanism of DWNTs in these processes, it is important to study relationship between the inner and outer tube of DWNTs.

In this paper, the van der Waals potential energy of DWNTs of various relative chirality pairings is examined. In addition, the formation process of a DWNT from a peapod by heat treatment is studied by classical molecular dynamics simulation. Finally, an explanation of wider mean distance between inner and outer tube of a DWNT than that found in other multi-layer grapheme sheet structure is proposed base on the above two results.

Nomenclature

ε : potential parameter (related to well depth)

σ : potential parameter (van der Waals radius)

$a_{c\text{-}c}$: intermolecular distance between two carbon atoms

$\boldsymbol{a}_1$, $\boldsymbol{a}_2$: real space unit vector of the hexagonal lattice

d_t : diameter of nanotube

B_{ij}^* : valence function

b : potential parameter

D_e : depth of potential

E_b : binding energy

f : cutoff function

R_e : interatomic distance of equilibrium

r_{ij} : distance between atoms i and j

S : potential parameter

V_A : attractive force term

V_R : repulsive force term

β : potential parameter

δ : potential parameter

2. Chirality dependence of potential energy of DWNTs

Here, the dependence of the potential energy of DWNT on the chirality of the inner and outer tube is examined. The interaction between the inner and outer tube is expressed using a standard 6-12 Lennard-Jones potential function:

$$U = 4\varepsilon\left\{\left(\frac{\sigma}{r}\right)^{12} - \left(\frac{\sigma}{r}\right)^{6}\right\}. \quad (1)$$

The parameters, ε = 2.5 meV and σ = 3.37 Å were used for describing the van der Waals potential between graphite layers per a carbon atom [22].

Firstly, the periodic stacking effect of the layers is focused on. Whereas a DWNT has only one interaction between the inner and outer tube (for an isolated tube), a MWNT has other periodic interactions from opposite and removed layers. Potential energies of 2 layer (non-periodic) and 8 layers in a periodic cell are compared using a grapheme sheet consisting of 1344 carbon atoms, with 60 Å side-length, as a layer. Figure 1 shows the potential energies per a carbon atom at various layer distances.

*[**Figure 1**]*

These energies were fitted by the following equation:

$$U = \frac{2}{3}\varepsilon\left\{\left(\frac{\sigma}{r}\right)^{10} - \frac{5}{2}\left(\frac{\sigma}{r}\right)^{6}\right\}. \quad (2)$$

Equation (2) represents the potential energy $U(r)$ as a function of the interlayer distance r (in one dimension) by integrating the potential energy from each carbon atom in the grapheme sheet. To describe this, the orders of the repulsive and the attractive terms are 10 and 6, respectively. The coefficients were determined by setting the potential energy equal to a minimum value ε at $r = \sigma$. The parameter σ in case of the 2 layers and 8 layers in a periodic cell was 3.357 Å and 3.323 Å, respectively. The difference is only about 0.03 Å. Moreover, the parameter ε (a measure of the depth of the potential well) of the 8 periodic layers is about twice that of the 2 layers. Hence, it is difficult to explain the wider interlayer spacing of DWNTs from just the non-periodic effect.

Secondly, the chirality dependence of potential energy of a DWNT is examined. The structure of a SWNT is specified by the chiral index (n,m) [11].

$$(n,m) = n\boldsymbol{a}_1 + m\boldsymbol{a}_2 \quad (3)$$

$$(\boldsymbol{a}_1,\boldsymbol{a}_2) = (\frac{3}{2},\frac{\sqrt{3}}{2})a_{\mathrm{C-C}} \quad (4)$$

The diameter of a SWNT d_t is determined by the real space unit vector of the hexagonal lattice $(\boldsymbol{a}_1,\boldsymbol{a}_2)$ and chiral index (n,m).

$$d_t = \frac{\sqrt{3}a_{\mathrm{C-C}}}{\pi}\sqrt{n^2 + nm + m^2} \quad (5)$$

SWNTs of (n,n) and $(n,0)$ are classified as either armchair nanotubes and zigzag nanotubes, respectively. These types have mirror symmetry. Other SWNTs are classified as chiral nanotubes, and have helical symmetry. The unit length of axial direction T can

be also determined by the real space unit vector of the hexagonal lattice and chiral index.

$$T = \left| t_1 \boldsymbol{a}_1 + t_2 \boldsymbol{a}_2 \right| \tag{6}$$

$$t_1 = \frac{2m+n}{d_R}, \quad t_2 = -\frac{2n+m}{d_R} \tag{7}$$

The constant d_R is the greatest common divisor of ($2m+n$) and ($2n+m$) [11]. The index (t_1,t_2) of armchair and zigzag nanotubes are (1,-1) and (1,-2), respectively. In the case of chiral nanotubes, it depends on the chiral index. For example, (t_1,t_2) of a (5,4) nanotube is (13,-14), which shows that the unit length of axial direction of this chiral tube is much longer than that of the armchair or zigzag tube.

Saito *et al.* [23] examined the stable structure of a DWNT for various chirality pairs in the case where the diameter of outer tube is less than 2 nm using a unit cell of finite length. The periodic cell condition for describing the infinite tube can be made by using the greatest common divisor of unit length of the inner and outer tube. However, the length of periodic unit cell is much longer in the case that both inner and outer tubes are chiral. In this study, only armchair (10,10) tube and zigzag (18,0) tube, which have almost same diameter (about 13.5 Å), are used as the outer tube. All tubes that have smaller diameter than the outer tube are examined as the inner tube. The potential energy of these DWNTs is calculated using the 6-12 Lennard-Jones potential function, Eq. (1), in a following way. The intermolecular distance between two carbon atoms $a_{c\text{-}c}$ is set to 1.42 Å in this study. The outer tube is rotated and translated in the range of the axial symmetry (36° for (10,10), 20° for (18,0)) and translational symmetry (2.45 Å for (10,10), 4.5 Å for (18,0)), respectively. Figure 2 shows the potential energy map of the (10,10)-(5,5) DWNT. Maxima and minima can be observed periodically in the map, however the range between these points is only 0.015 meV. Hence the DWNT will not

stay at the minimum point, and has possibility for relative rotational motion of the tubes at the room temperature (cf. k_BT = 25.7 meV/atom at 298 K).

*[**Figure 2**]*

Figure 3 shows the minimum point in the potential energy map of various combinations of DWNTs plotted as a function of the intertube distance. The most stable intertube distance is about 3.3 Å in case of both types of outer tubes (armchair and zigzag). Moreover, there is no point that appears to be singularly stable by a special combination of the chirality of the inner and outer tubes. These tendencies are in accordance with the results obtained by Saito *et al.* [23].

*[**Figure 3**]*

In summary, it is difficult to explain the reason for the larger mean distance between the inner and outer tube in a DWNT from only the van der Waals force between tubes.

3. Molecular Dynamics Simulation

Next, the generation process of a DWNT from a peapod via heat treatment is modelled by a classical molecular dynamics method, and the reason for a larger mean intertube distance is investigated by such a kinetic approach. Initial condition for the peapod simulations was 5 C_{60} molecules encapsulated in a (10,10) SWNT of length 68.75 Å (Fig. 4).

*[**Figure 4**]*

The SWNT has a periodic boundary condition and is fixed. The Brenner potential [24] is used for covalent bonding for carbon atoms in C_{60} molecules. In previous work, we have confirmed that the Brenner potential expressing the covalent bonding for a

nanotube accurately by the molecular dynamics simulation of formation process of a SWNT in a laser-oven technique [25,26].

The total potential energy of the system E_b by a Brenner potential is expressed as the sum of the bonding energy of each bond between carbon atom *i* and *j*:

$$E_b = \sum_i \sum_{j(i>j)} \left[V_R(r_{ij}) - B_{ij}^* V_A(r_{ij}) \right]. \tag{8}$$

$V_R(r)$ and $V_A(r)$ are repulsive and attractive force terms, respectively. The Morse-type form with a cutoff function $f(r)$ expressed these terms:

$$V_R(r) = f(r) \frac{D_e}{S-1} \exp\left\{ -\beta\sqrt{2S}(r - R_e) \right\} \tag{9}$$

$$V_A(r) = f(r) \frac{D_e S}{S-1} \exp\left\{ -\beta\sqrt{2/S}(r - R_e) \right\} \tag{10}$$

$$f(r) = \begin{cases} 1 & (r < R_1) \\ \frac{1}{2}\left(1 + \cos\frac{r - R_1}{R_2 - R_1}\pi \right) & (R_1 < r < R_2) \\ 0 & (r > R_2) \end{cases} \tag{11}$$

The effect of the bonding condition of each atom is taken into account through the B_{ij}^* term which is a function of angle θ_{ijk} between bond *i*-*j* and *i*-*k*:

$$B_{ij}^* = \frac{B_{ij} + B_{ji}}{2} \tag{12}$$

$$B_{ij} = \left(1 + \sum_{k(\neq i,j)} \left[G_C(\theta_{ijk}) f(r_{ik}) \right] \right)^{-\delta} \tag{13}$$

$$G_C(\theta) = a_0 \left(1 + \frac{c_0^2}{d_0^2} - \frac{c_0^2}{d_0^2 + (1 + \cos\theta)^2} \right) \tag{14}$$

The following potential parameters [24] were used:

D_e = 6.325 eV, S = 1.29, β = 1.5 Å^{-1}, R_e = 1.315 Å, δ = 0.80469, a_0 = 0.011304, C_0 = 19, d_0 = 2.5, R_1 = 1.7 Å, R_2 = 2.0 Å.

In addition, the 6-12 Lennard-Jones potential, Eq. (1), with the parameters ε = 2.5 meV and σ = 3.37 Å was used between the carbon atoms of the SWNT and those of the C_{60} molecules. The velocity Verlet method was employed to integrate the classical equation of motion with a time step of 0.5 fs. In order to observe the growth process of a longer time-scale within the computational limit, the controlled temperature was much higher than the experimental conditions [19]. This is compensated for by a very rapid cooling technique using the Berendsen thermostat [29], with the rotational and vibrational temperature of the system controlled independently. The actual simulation temperature does not correspond directly with that in the experimental study, however the relationship between these temperatures is examined in our other papers [31,32].

Figure 5 shows snapshots of the growth process of the DWNT from the peapod by a 100 ns molecular dynamics calculation at 3000 K. The outer tube is not shown for clarity. In the first stages, the fullerenes polymerize. After that, bond switching with a long time scale occurs, and these fullerenes change to a peanut-like structure. Finally, a transition to an almost nanotube-like structure is observed.

[Figure 5]

In the same way, the DWNT growth process at various temperatures from 1500 K to 4000 K was examined. Figure 6 shows the time series of the mean distance between inner and outer tube at various temperatures. The mean diameter of inner tube-like structure was determined by taking an average of positions of all carbon atoms except those in the cap structure at the edges of the tubes.

[Figure 6]

Though the inner fullerenes stop changing in the peanut-like structure at less than 2500 K, an ellipse structure, which is regarded as the next stage of the peanut-like structure, was observed at 3000 K. In that structure at 3000 K, the mean distance between inner

and outer tubes is about 3.6 Å, which is close to the distance observed in the experimental results [19]. In case of simulations at 3500 K and 4000 K, the original structure of C_{60} vanishes by the mechanism of frequent bond switching. It is expected that there are some energy barriers in the formation process from a peapod to a DWNT because the final shape depends on the temperature.

In general, the Stone-Wales (SW) transformation [20] is well known for the bond-switching path of sp^2 bonds of carbon atoms in fullerenes and nanotubes, and continuous SW transformation can lead to structural phase changes. In previous work, the SW transformation was observed at less than 3000 K using a Brenner potential over the time scale of a typical molecular dynamics simulation [31,32]. In this study, the mean distance between two layers of a DWNT corresponds to the experimental result at 3000 K that was the highest temperature at which SW transformation was observed in the simulation. In case of temperatures over 3500 K, the mean distance converges to about 3.4 Å. It is because of an abnormal path of bond switching that the original structure of the fullerenes vanishes and carbon atoms take optimum position by van dear Waals force that make the distance at 3.4 Å. Hence, it is difficult for the mean distance of two layers of a DWNT generated by heat treatment of a peapod to take only 3.4 Å by the SW transformation. This explains why the mean distance takes about 3.6 Å in the experimental results, where the transformation must occur by SW transformation.

Finally, the sensitivity of mean distance to the Lennard-Jones potential parameters must be considered. In above simulation, the mean distance takes optimum of the 6-12 Lennard-Jones potential at temperatures only over 3500 K. However, the mean distance of a DWNT generated from a peapod via continuous SW transformation is not affected by the Lennard-Jones potential, rather it is affected by the structure of original fullerene.

In summary, the Lennard-Jones potential parameters do not appear to be critical in this formation process.

4. Conclusions

The generation process of a DWNT from a peapod was studied by classical molecular dynamics simulation. A continuous structural change from fullerene to polymerized fullerene, a peanut-like structure and almost nanotube-like structure was observed. An energy barrier was observed when the structure changes. In addition, the chirality dependence of the potential energy of a DWNT was examined using a 6-12 Lennard-Jones potential. The potential energy depends only on the distance between the two layers, not on the relative chirality of the inner and outer tubes. Hence, the larger average separation of the two tube layers in a DWNT than that witnessed in MWNTs or turbostratic graphite must be due to the kinetic path in formation process of DWNTs.

Acknowledgments

This work was partially supported by Grant-in-Aid for Scientific Research [No.13GS0019] from MEXT, Japan and Grant-in-Aid for JSPS fellow [No.15-11043]. The authors appreciate Dr. J.A. Elliott at University of Cambridge for useful discussion.

Literature Cited

1. Iijima S. Nature, Helical microtubes of graphitic carbon. Nature 1991;354:56-58.

2. Iijima S, Ichihashi T. Single-shell carbon nanotubes of 1-nm diameter. Nature 1993;363:603-605.

3. Saito R, Dresselhaus G, Dresselhaus MS. Physical Properties of Carbon Nanotubes. Imperial College Press; 1998. Chapter 3.

4. Thess A, Lee R, Nikoraev P, Dai H, Petit P, Robert J, Xu C, Lee YH, Kim SG, Rinzler AG, Colbert DT, Scuseria GE, Tománek D, Fischer JE, Smalley RE. Crystalline ropes of metallic carbon nanotubes. Science 1996;273:483-487.

5.Journet C, Maser WK, Bernier P, Louseau A, de la Chapelle ML, Lefrant S, Deniard P, Lee R, Fisher JE. Large-scale production of single-walled carbon nanotubes by the electric-arc technique. Nature 1997;388:756-758.

6. Dai H, Rinzler AG, Nikolaev P, Thess A, Colbert DT, Smalley RE. Single-wall nanotubes produced by metal-catalyzed disproportionation of carbon monoxide. Chem. Phys. Lett. 1996;260:471-475.

7. Maruyama S, Kojima R, Miyauchi Y, Chiashi S, Kohno M. Low-temperature synthesis of high-purity single-walled carbon nanotubes from alcohol. Chem. Phys. Lett. 2002;360:229-234.

8 Maruyama S, Miyauchi Y, Chiashi S, Kohno. M. Low-temperature generation of high-purity single-walled carbon nanotubes by alcohol CCVD technique. Trans JSME Ser B 2003;69-680:918-924.

9. Maruyama S. Synthesis of single-walled carbon nanotubes and characterization with resonant Raman scattering. Trans JSME Ser B 2003;69-682:1495-1502.

10. Murakami Y, Miyauchi Y, Chiashi S, Maruyama S. Characterization of single-walled carbon nanotubes catalytically synthesize from alcohol. Chem. Phys. Lett. 2003;374:53-58.

11. Murakami Y, Miyauchi Y, Chiashi S, Maruyama S. Direct synthesis of high-quality single-walled carbon nanotubes on silicon and quartz substrates. Chem. Phys. Lett. 2003;377:49-54.

12. Smith BW, Monthioux M, Lussi DE. Encapsulated C_{60} in carbon nanotubes. Nature 1998;396:323-324.

13. Rinzler, AG, Lie J, Dai H, Nikolaev P, Huffman CB, Rodríguez-Macías FJ, Boul PJ, Lu AH, Heymann D, Colbert DT, Lee RS, Fischer JE, Rao AM, Eklund PC, Smalley RE, Large-scale purification of single-wall carbon nanotubes: process, product, and characterization. Appl. Phys. A 1998;67:29-37.

14. Smith BW, Luzzi DE. Formation mechanism of fullerene peapods and coaxial tubes: a path to large scale synthesis. Chem. Phys. Lett. 2000;321:169-174.

15. Kataura H, Maniwa Y, Kodama T, Kikuchi K, Hirakawa K, Suenaga K, Iijima S, Suzuki S, Achiba Y, Krätschmer. High-yield fullerene encapsulation in single-wall carbon nanotubes. Synthesis Metals 2001;121:1195-1196.

16. Hirahara K, Bandow S, Suenaga K, Kato H, Okazaki T, Shinohara H, Iijima S. Electron diffraction study of one-dimensional crystals of fullerenes. Phys. Rev. B 2001;64:115420-1-115420-5.

17. Hirahara K, Suenaga K, Bandow S, Kato H, Okazaki T, Shinohara H, Iijima S, One-dimensional metallofullerene crystal generation inside single-walled carbon nanotubes. Phys. Rev. Lett. 2000;85:5384-5387.

18. Smith BW, Monthioux M, Luzzi DE. Carbon nanotube encapsulated fullerenes: a unique class of hybrid materials, Chem. Phys. Lett. 1999;315:31-36.

19. Bandow S, Takizawa M, Hirahara K, Yudasaka M, Iijima S. Raman scattering study of double-wall carbon nanotubes derived from the chains of fullerenes in single-wall carbon nanotubes. Chem. Phys. Lett. 2001;337:48-54.

20. Sugai T, Yoshida H, Shimada T, Okazaki T, Shinohara H. New synthesis of high-quality double-walled carbon nanotubes by high-temperature pulsed arc discharge. Nano letters 2003;3:769-773.

21. Hiraoka T, Kawakubo T, Kimura J, Taniguchi R, Okamoto A, Okazaki T, Sugai T, Ozeki Y, Yoshikawa M, Shinohara H. Selective synthesis of double-wall carbon nanotubes by CCVD of acetylene using zeolite supports. Chem. Phys. Lett. 2003;382:679-685.

22. Maruyama S, Kimura T. Molecular dynamics simulation of hydrogen storage in single-walled carbon nanotubes, Proc. ASME Heat Transfer Division 2000, p 405-409, 2000.

23. Saito R, Matsuo R, Kimura T, Dresselhaus G, Dresselhaus MS. Anomalous potential barrier of double-wall carbon nanotube. Chem. Phys. Lett. 2001;348:187-193.

24. Brenner DW. Empirical potential for hydrocarbons for use in simulating the chemical vapor deposition for diamond films. Phys. Rev. B 1990;42:9458-9471.

25. Yamaguchi Y, Maruyama S. A molecular dynamics study on the formation of metallofullerene. Eur. Phys. J. D 1999;9:385-388.

26. Yamaguchi Y, Maruyama S, Shin-ichi Hori. Molecular dynamics simulation of formation of metal-containing fullerene. Trans JSME Ser B 1999;65-630:431-436.

27. Shibuta Y, Maruyama S. Molecular dynamics simulation of generation process of SWNTs. Physica B 2002;323:187-189.

28. Shibuta Y, Maruyama S, Molecular dynamics in formation process of single-walled carbon nanotubes. Trans JSME Ser B 2002;68-675:3087-3092.

29. Berendsen HJC, Postma JPM, van Gunsteren WF, DiNola A, Haak JR. Molecular dynamics with coupling to an external bath. J. Chem. Phys. 1984;81:3684-3690.

30. Stone AJ, Wales DJ. Theoretical studies of icosahedral C_{60} and some related species. Chem. Phys. Lett. 1986;128:501-503.

31. Maruyama S, Yamaguchi Y. A molecular dynamics if the formation process of fullerene (2nd report, annealing to the perfect C_{60} structure). Trans JSME Ser B 1997;63-611:2405-2412.

32. Maruyama S, Yamaguchi Y, A molecular dynamics demonstration of annealing to a perfect C_{60} structure. Chem. Phys. Lett. 1998;286:343-349.

Figure and Table Captions

Fig. 1. Potential energy of graphite with L-J potential.

Fig. 2. Chirality Matching of DWNT ((5,5) in (10,10))

Fig. 3. Van der Waals potential energy of DWNTs.

(a) outer tube (10,10)

(b) outer tube (18,0)

Fig. 4. Initial conditions for peapod simulations, $(C_{60})_5$@(10,10).

Fig. 5. Snapshots of formation process from a peapod to a DWNT

Fig. 6. Mean distance between inner and outer tube.

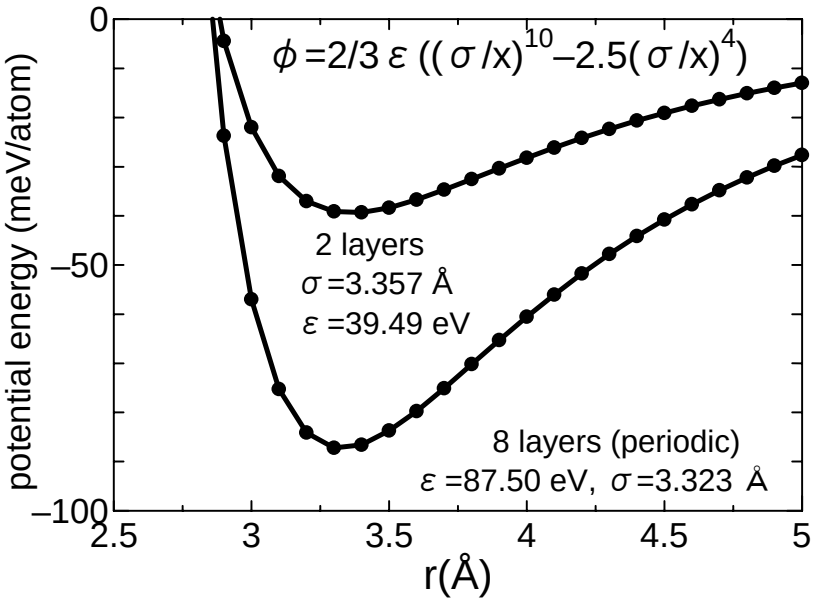

Fig. 1. Potential energy of graphite with L-J potential.

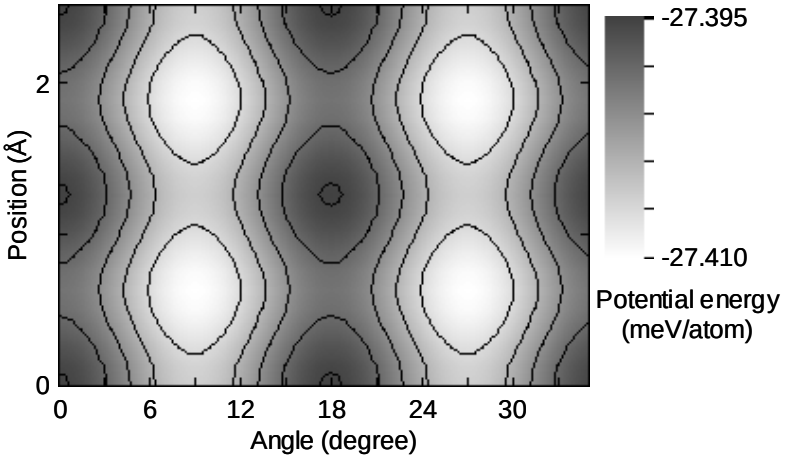

Fig. 2. Chirality Matching of DWNT ((5,5) in (10,10))

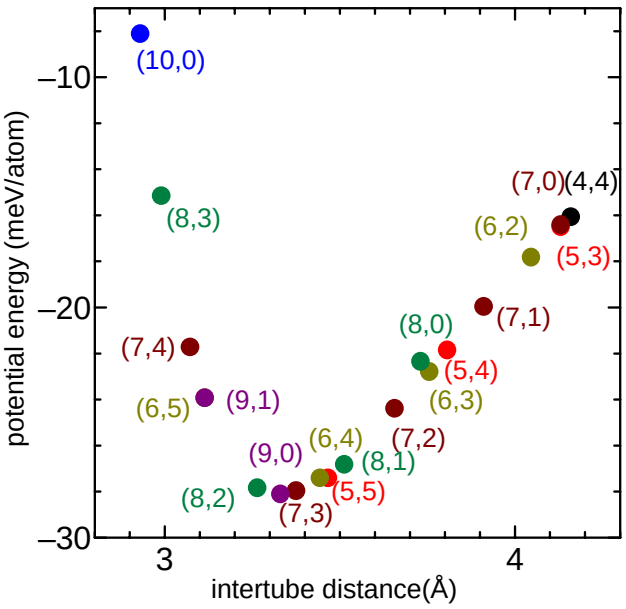

(a) outer tube (10,10)

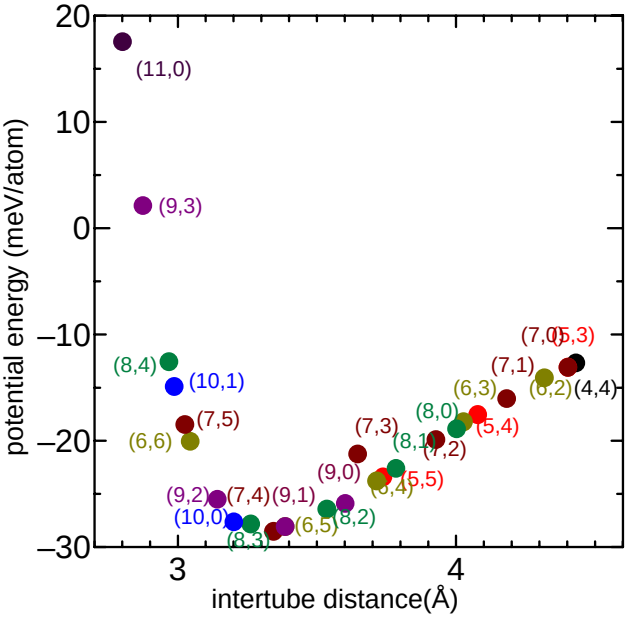

(b) outer tube (18,0)

Fig. 3. Van der Waals potential energy of DWNTs.

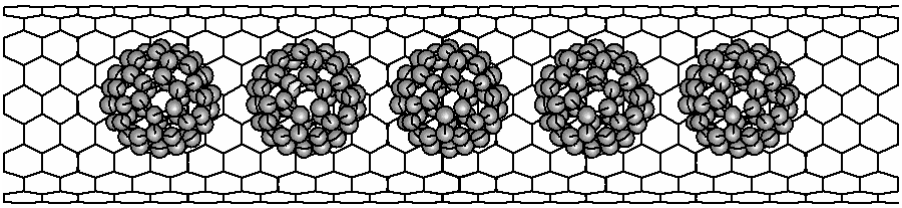

Fig. 4. Initial conditions for peapod simulations, $(C_{60})_5$@(10,10).

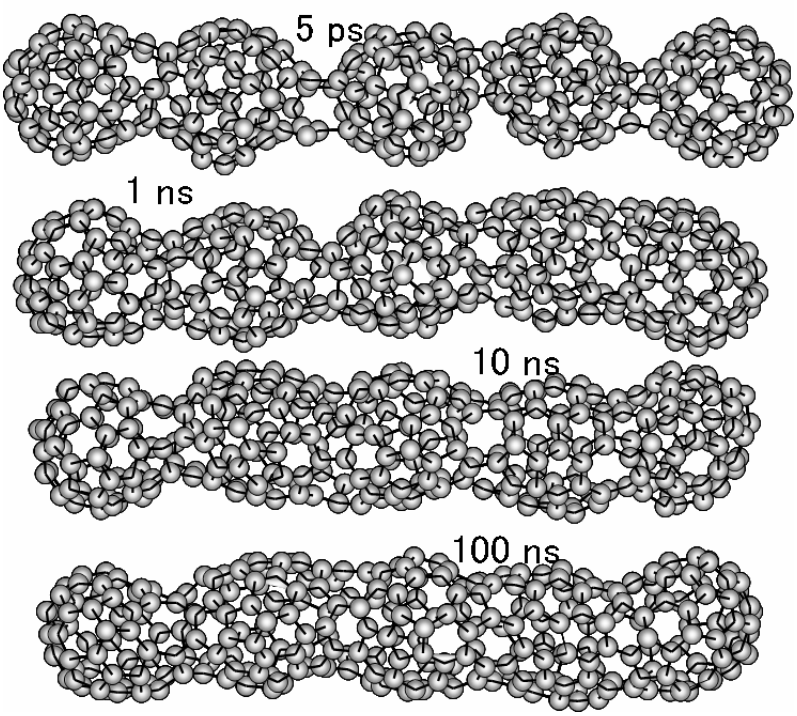

Fig. 5. Snapshots of formation process from a peapod to a DWNT

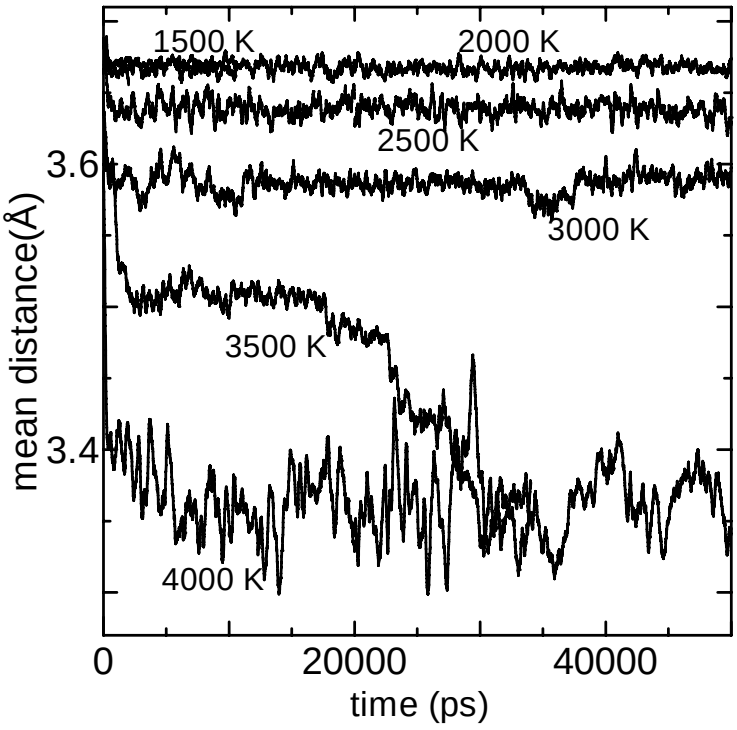

Fig. 6. Mean distance between inner and outer tube.